Thermochimica Acta, 106 (1986) 141–154
Elsevier Science Publishers B.V., Amsterdam – Printed in The Netherlands

SOME FEATURES OF THERMAL BEHAVIOR OF $Na_5P_3O_{10} \cdot 6H_2O$

V.M. GALOGAŽA[1], E.A. PRODAN[2], V.A. SOTNIKOVA-YUZHIK[2], D.U. SKALA[1], N.V. BULAVKINA[2] and S.I. PYTLEV[2]

[1] *University of Belgrade, Faculty of Technology and Metallurgy, Belgrade (Yugoslavia),*
[2] *Institute for General and Inorganic Chemistry, Academy of Sciences of Belorussian SSR, Minsk (U.S.S.R.)*

(Received 21 February 1986)

ABSTRACT

Using DSC, TG, EM, quantitative TLC and XRD methods, the iso- and non-isothermal behavior of the sodium chain-triphosphate hexahydrate, $Na_5P_3O_{10} \cdot 6H_2O$, has been investigated in vacuum and in flows of different gases. Its specificity and some differences from the thermal behavior of the sodium cyclo-triphosphate hexahydrate, $Na_3P_3O_9 \cdot 6H_2O$, are discussed. On heating, successive processes take place: a dehydration of the $Na_5P_3O_{10} \cdot 6H_2O$ through a series of steps, involving a degradation step to the mono- and diphosphates, which cannot react with the gaseous ammonia, and their recondensation to $Na_5P_3O_{10}$-II; the transition of $Na_5P_3O_{10}$-II into $Na_5P_3O_{10}$-I, and melting of $Na_5P_3O_{10}$-I with anion rearrangement. At premelting and melting stages of $Na_5P_3O_{10}$-I, some effects, sensitive to the material of the pan, were observed. These effects have been explained by an unconventional change of physical state and the anion composition of the sample.

INTRODUCTION

For comparison of the stability, reactivity and other properties of the chain and cyclic triphosphates in different aggregate states (water solution, crystalline, amorphous, vitreous (glassy) phase) it is interesting to compare the thermal characteristics of salts of the same type which are found in just the same state, especially for the crystalline forms of $Na_5P_3O_{10} \cdot 6H_2O$ and $Na_3P_3O_9 \cdot 6H_2O$. On heating to $t = 100\,°C$, the salt with cyclic anion relatively easily loses crystal water with no rupture of the anion cycle [1]:

$$Na_3P_3O_9 \cdot 6H_2O(\text{cryst.}) \rightarrow Na_3P_3O_9(\text{cryst.}) + 6H_2O(g)$$

According to a quantitative X-ray analysis [2], the rate of crystallization of the anhydrous cyclotriphosphate is essentially no different from the rates of initial crystal lattice destruction and dehydration, which take place in a kinetic regime and are not complicated by the diffusion processes. Moreover, if reaction with a rupture of the anion cycle is required, the dehydration process must be realized at a relatively high vapor pressure of water and

0040-6031/86/$03.50

ammonia. In these conditions, the intermediate monohydrate, $Na_3P_3O_9 \cdot H_2O$, is formed, which loses its crystalline water through a cyclic rupture and with ammonization of the dehydration products.

On the other hand, during heating of $Na_5P_3O_{10} \cdot 6H_2O$, anhydrous salt is almost unobtainable without the intermediate destruction of the chain-triphosphate anion. The sodium chain-triphosphate represents an industrial product, and the loss of its hydration water without anion destruction is an application problem which needs to be solved; much time has already been devoted to it [3–5]. On thermal treatment of the hexahydrate, $Na_5P_3O_{10} \cdot 6H_2O$, a high yield of anhydrous sodium triphosphate was obtained [6], but it is not clear whether this was formed directly, or via the degradation mechanism [7].

EXPERIMENTAL

In this work the features of iso- and non-isothermal behavior of $Na_5P_3O_{10} \cdot 6H_2O$, compared to that of $Na_3P_3O_9 \cdot 6H_2O$, are investigated and discussed. The sample of chromatographically pure $Na_5P_3O_{10} \cdot 6H_2O$, which was used in the experimental work, was produced by five-fold recrystallization (the diameter of the crystalline particles was $D = 0.02$–0.2 mm) from which on mild grinding a powder sample was obtained ($D = 0.002$–0.02 mm). For comparison, the thermal behavior of the chromatographically pure $Na_3P_3O_9 \cdot 6H_2O$ (particle size $D = 0.01$–0.3 mm), obtained according to ref. 1, as well as low-temperature ($Na_5P_3O_{10}$-II) and high-temperature ($Na_5P_3O_{10}$-I) crystalline forms of the anhydrous chain-triphosphate, were also investigated.

The last two forms were obtained on thermal treatment of the hexahydrate $Na_5P_3O_{10} \cdot 6H_2O$ in flowing water vapor at $t = 450 \pm 10°C$ and $t = 550 \pm 10°C$, respectively. According to data obtained from TLC analysis (KTH-0.1 equipment set for thin layer chromatography), and quantitative XRD analysis data (DRF-2.0 diffractometer, CuK_α irradiation) according to ref. 8, anhydrous samples are not contaminated by other anionic forms or/and other crystalline phases. Two anhydrous samples represent a crystalline powder with $D = 0.005$–0.02 mm and specific surface of $S = 3 \pm 1$ m^2 g^{-1}.

Some experiments were carried out under vacuum using a high vacuum apparatus with a quartz spiral-microbalance (sensitivity 0.83 mg mm^{-1}; mass of the sample, $m \approx 20$ mg). For the experiments performed in flowing nitrogen, a Perkin-Elmer Thermal Analysis Lab 1 with DSC-2 Scan Auto Zero unit (nitrogen flow rate 37 cm^3 min^{-1}) and TGS-2 Model FDC-1 (nitrogen flow rate 17 cm^3 min^{-1}) were used. The nitrogen was dried to 20–30 ppm of impurity or saturated with water and ammonia vapors, passed through 25% aqueous ammonia solution at 25°C and then dried. The powder sample ($m = 4$–18 mg) was placed in standard Perkin-Elmer platinum, gold or graphite pans and then heated at a constant heating rate (non-isothermal experiments) or rapidly heated at a heating rate of HR = 160 °C min^{-1} up to the defined temperature and then kept at constant temperature to ± 0.1°C (isothermal experiments). Samples were prepared for XRD analysis ($m = 1$–2 g) in a separate series of experiments. Electron microscopic investigations were carried out with an electron microscope (Philips E.M. 300) following the graphite-replica method.

For the investigation of the thermal behavior of $Na_3P_3O_9 \cdot 6H_2O$ in an ammonia atmosphere, a high vacuum apparatus was used, and after obtaining a vacuum, the ammonia was added at a definite pressure.

RESULTS AND DISCUSSION

During heating of $Na_3P_3O_9 \cdot 6H_2O$, continual evolution of water vapor occurs, expressed on the DSC curve as one dehydration peak with a maximum at $t = 60$ °C. The second observable effect is the melting of $Na_3P_3O_9$. From the TLC data, in this temperature range there are no traces of anion decyclization. Under suppressed evolution of water vapor, for example, during the heating of an encapsulated sample, the whole endo-effect of dehydration is divided into two or three smaller effects. This is because dehydration proceeds through the formation of intermediate crystal hydrates.

The $Na_5P_3P_{10} \cdot 6H_2O$ dehydration effect also has a complex form on the DSC curve (Fig. 1). In this case intermediate crystal hydrates are not characteristic, indicating that the multistep evolution of water is caused by other factors.

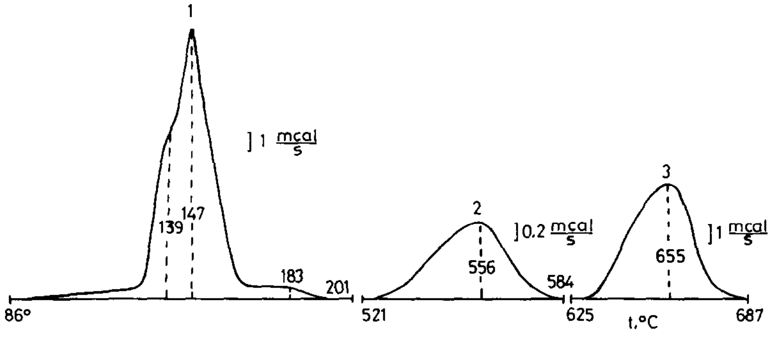

Fig. 1. DSC curves for the heating process of $Na_5P_3O_{10} \cdot 6H_2O$ ($D = 0.02$–0.2 mm) in a dry nitrogen atmosphere. (1) Dehydration, HR = 20 K min^{-1}, $m = 4.83$ mg; (2) transformation $Na_5P_3O_{10}$-II → $Na_5P_3O_{10}$-I, HR = 20 K min^{-1}, $m = 4.83$ mg; (3) melting process, HR = 80 K min^{-1}, $m = 11.56$ mg.

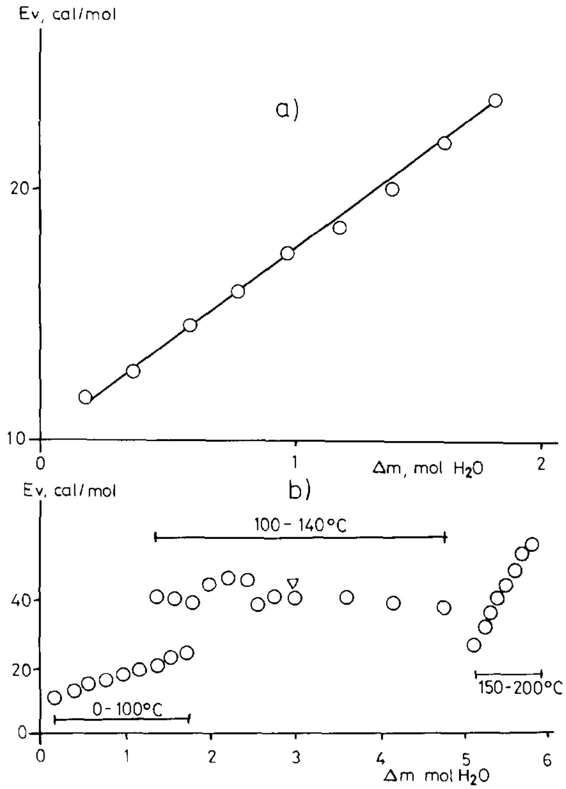

Fig. 2. Change of E_v during the dehydration process of $Na_5P_3O_{10}\cdot 6H_2O$ ($D = 0.002$–0.02 mm) in a vacuum at: $t = 0$–100°C (a) and $t = 0$–200°C (b); $P = 10^{-4}$ hPA, $m = 20$ mg; isothermal experiments.

It is known [4,7] that for a mass loss $\Delta m \leqslant 2$ mol H_2O, the hexahydrate $Na_5P_3O_{10}\cdot 6H_2O$ loses water reversibly, and retains the same X-ray diffraction pattern as that at the beginning of the dehydration process. Moreover, the first part of the crystal water ($\Delta m < 0.6$ mol H_2O) is released in a kinetic regime, and the second (0.6 mol $< \Delta m \leqslant 2$ mol H_2O) in a diffusion regime with growing diffusion resistance, as a result of the increased thickness of the solid reaction product layer which covers the crystal surface. The slowly and rapidly increasing sections of the DSC curve up to inflection point at $t = 139$°C (Fig. 1) correspond to these dehydration stages.

When the process is carried out under vacuum both stages end at $t \leqslant 100$°C. Increasing diffusion resistance occurred such that the effective activation energy for the dehydration process gradually increased. The change in effective activation energy, E_v, which is obtained from the temperature dependence of the rates of isothermal dehydration at fixed Δm, is shown in Fig. 2a. The straight-line function E_v versus Δm could be explained in the following manner: in a certain range of Δm change, the

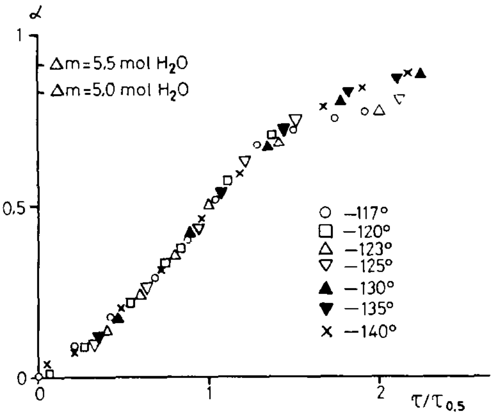

Fig. 3. Kinetic curves for the isothermal dehydration process of $Na_5P_3O_{10}\cdot 6H_2O$ ($D=$ 0.02–0.2 mm) in a dry nitrogen atmosphere; for $t=125\,°C$ the half-time period, $\tau_{0.5}=17$ min.

structure and anion composition of the product layer do not change and only its thickness increases, producing a higher partial pressure of water, p_{H_2O}, in the reaction zone. Extrapolation to $\Delta m=0$ and $p_{H_2O}=0$ gives values of E_v which are almost the same as the heat of vaporization of ice. The size of the sample particles does not affect the general feature of this process, but only influences the proportion of water removed in the first or second stages.

The effect with a maximum at $t=147\,°C$ (Fig. 1) corresponds to the removal of the main part of the water ($\Delta m=2.0$–5.0 mol H_2O) with a simultaneous high degradation of the chain anion. From data of TLC analysis the sample with $\Delta m=4.6$ mol H_2O contains 27.6% of the phosphorus in the form of monophosphate (P_1), 62.8% in the form of diphosphate (P_2) and 9.6% in the form of chain-triphosphate (P_3). At this stage of dehydration, the value of E_v, after a stepwise change near Δm = 2 mol H_2O, does not change as a function of the mass change Δm. This value of E_v then corresponds to the energy of bond breaking of the P–O bridge. It is only slightly sensitive to the nature and composition of the gas atmosphere. In Fig. 2b at $\Delta m=3$ mol H_2O an experimental point (▽) is shown which corresponds to dehydration in flowing nitrogen. In Fig. 3 the kinetic curves, in the form of the dependence of the degree of conversion, α, on reduced time, $\tau/\tau_{0.5}$ are shown. They have a typical S-shape, which is characteristic of the analogous curves of the dehydration of $Na_5P_3O_{10}\cdot 6H_2O$ in vacuum, and which in the final stage become almost horizontal at Δm = 5.0–5.5 mol H_2O.

The residual water, which is bound in the form of P–OH groups, represents a small part of the starting 6 moles of water. This quantity of water participated in a hydrolytic rupture of the P–O bridge bonds and is removed in one of the shemes of anion recondensation:

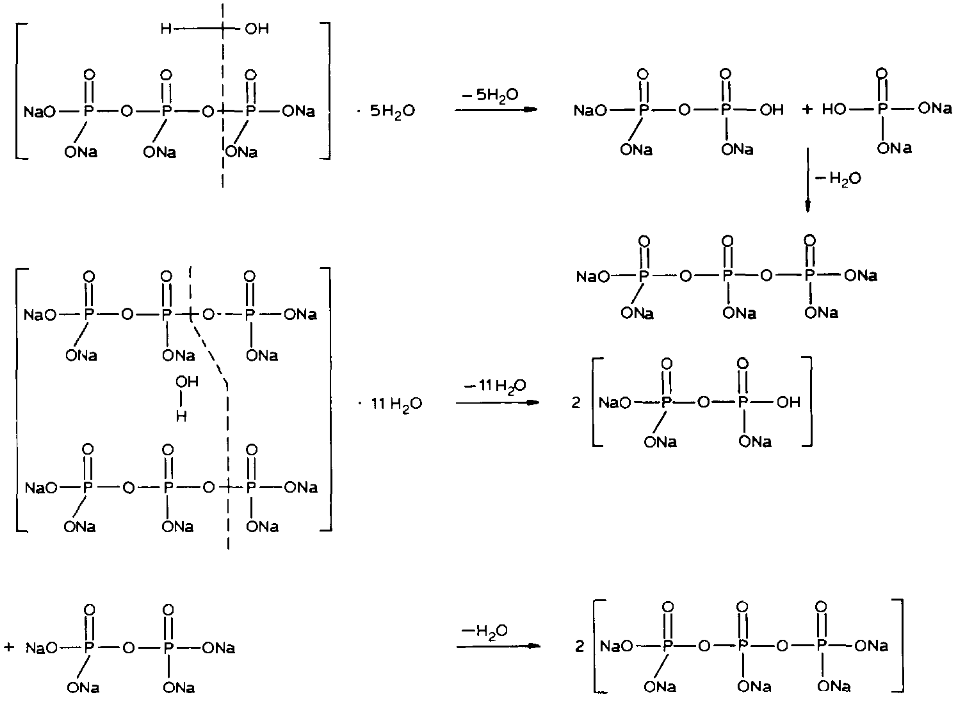

At the stage of anion recondensation ($\Delta m = 5.0$–6.0 mol H_2O), which both in vacuum and flowing nitrogen, finished at $t = 190$–$200\,°C$, the effective activation energy undergoes a second stepwise change in the temperature range $t = 140$–$150\,°C$, and after that almost linearly increases with increasing Δm (Fig. 2b). This stage corresponds to the smooth decreasing section of the dehydration effect at $t = 160$–$190\,°C$ (Fig. 1). The sample heated in flowing nitrogen to 200 °C represents the low-temperature forms (II) of the anhydrous sodium chain-triphosphate; from the TLC data its composition is: 3.6% P_1, 4.4% P_2 and 92.0% P_3. A difference between the thermal behavior of $Na_5P_3O_{10} \cdot 6H_2O$ and $Na_3P_3O_9 \cdot 6H_2O$ is not limited only to this aspect. Both salts are also different as to the possibility of the P–OH groups, which are formed on hydrolytic rupture of the P–O bonds, to react with gaseous ammonia.

Products of the degradation of chain-triphosphate practically do not interact with ammonia, as is shown by the TG curve obtained during heating of $Na_5P_3O_{10} \cdot 6H_2O$ in flowing nitrogen and in a mixture of N_2 and NH_3. Both curves are identical (Fig. 4). Meanwhile, TG curves obtained during heating of $Na_3P_3O_9 \cdot 6H_2O$ in atmospheres of dry and moist ammonia are different to those in a vacuum. The difference is a mass growth effect at $t = 170$–$200\,°C$ (Fig. 5), which is caused by the formation of the intermediate monohydrate $Na_3P_3O_9 \cdot H_2O$ that loses water with rupture of the

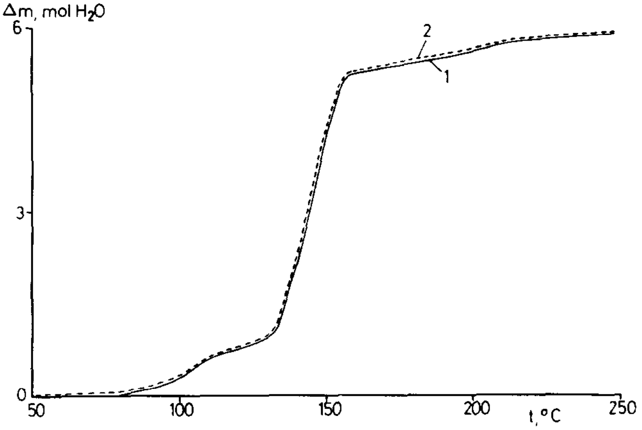

Fig. 4. TG curve for the heating process of $Na_5P_3O_{10}\cdot 6H_2O$ ($D = 0.02$–0.2 mm, heating rate $= 5$ K min^{-1}), in flowing nitrogen. (1) Dry nitrogen, $m = 11.46$ mg; (2) gas mixture $N_2 + NH_3$, $m = 10.66$ mg.

anion cycle and with ammonization of the acid chain-triphosphate formed. In general, these results correspond with the data obtained in the Institute of General and Inorganic Chemistry (Minsk), according to which the reaction of ammonization is not characteristic of the acid sodium and potassium orthophosphates, but is characteristic of the acid chain-triphosphate of these metals.

The effect with a maximum at $t = 556\,°C$ (Fig. 1) corresponds to the transition $Na_5P_3O_{10}$-II $\rightarrow$ $Na_5P_3O_{10}$-I, which is in accordance with the literature data [4], and could not be associated with a simple reversible polymor-

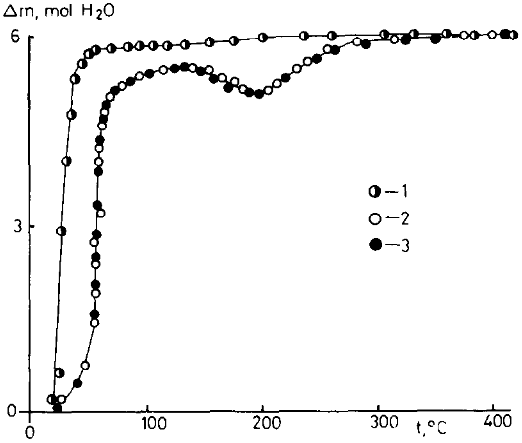

Fig. 5. TG curve for the heating process of $Na_3P_3O_9\cdot 6H_2O$ (HR = 2 K min^{-1}, $m = 50$ mg). (1) Vacuum, $P = 10^{-4}$ hPa, (2) atmosphere of dry ammonia, $P_{NH_3} = 1000$ hPa, (3) atmosphere of moist ammonia, $P_{NH_3} = 975$ hPa, $P_{H_2O} = 25$ hPa.

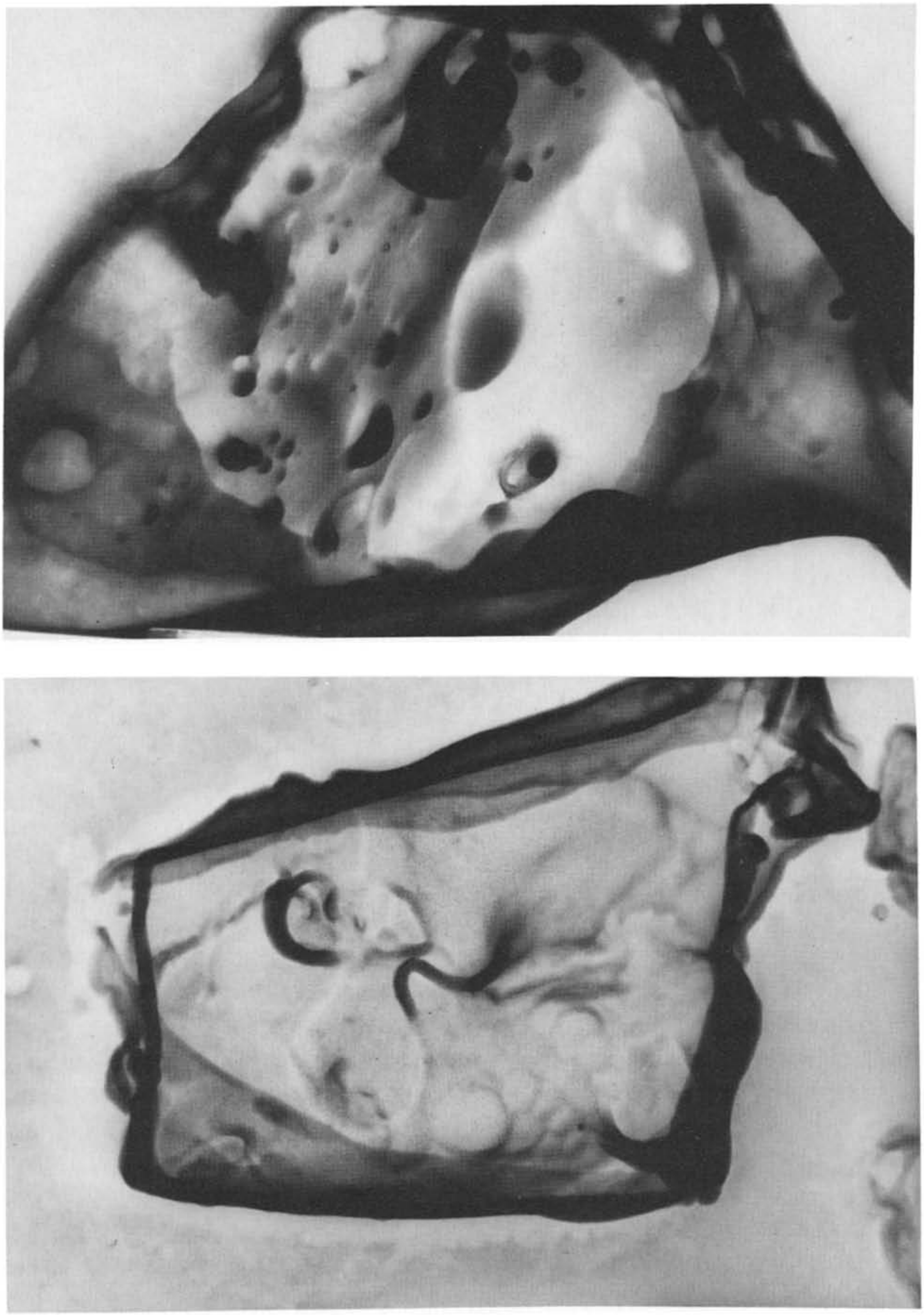

Fig. 6. Electron microscopic picture of the crystal particles of forms I and II of the sodium chain-triphosphate, obtained by heating $Na_5P_3O_{10} \cdot 6H_2O$ ($D = 0.02$–0.2 mm) in flowing dry nitrogen to $t = 350$–400°C (II) and $t = 590$–600°C (I) (magnification ×33000).

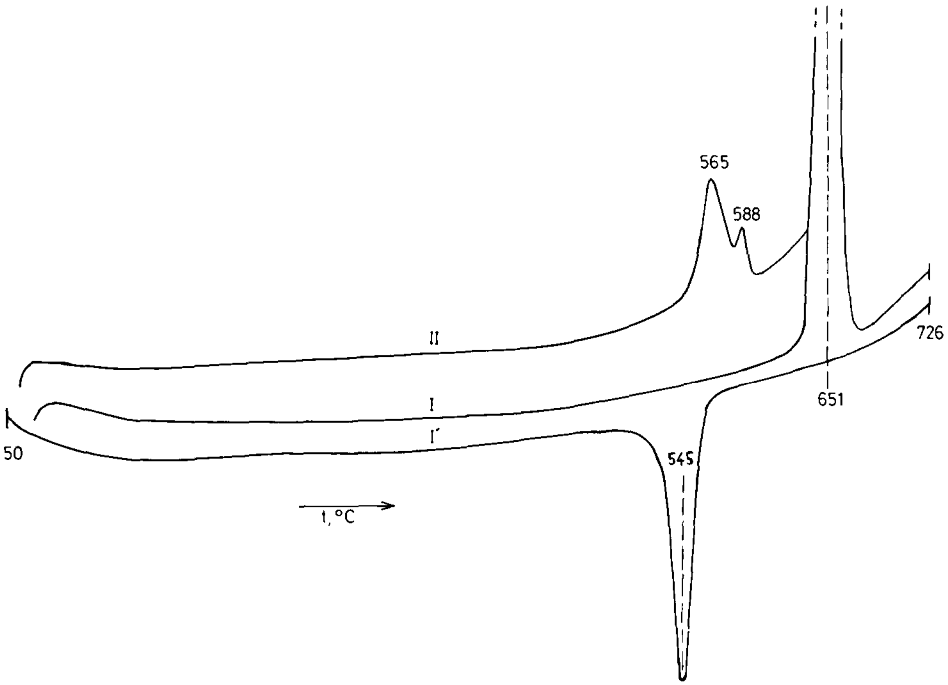

Fig. 7. DSC curves for the heating process of $Na_5P_3O_{10}$-I and $Na_5P_3O_{10}$-II in a dry nitrogen flow: (I) HR = 80 K min^{-1}, $m = 8.35$ mg; (I′) cooling rate; CR = 80 K min^{-1}; (II) HR = 40 K min^{-1}; $m = 9.92$ mg.

phic transformation. For this unusual effect, it is usually characteristic that form I, only changes once on cooling into form II with self-disintegration. The second time, this transformation into form II was not obtained with the same sample. Besides the self-disintegration, a stabilization effect during the cooling process of form I affected some admixtures. In our case, form I is not essentially different from form II with respect to the content of unreacted components as admixtures (after the heating process to $t = 597$ °C the sample consists of 2.3% P_1, 2.9% P_2 and 94.8% P_3), but it is different in that its particles have a porous structure (Fig. 6). It was apparent that this porosity has a stabilization effect on form I as well as promoting self-disintegration.

In some cases a splitting of the II → I effect is observed, for example during heating of the TLC-pure and XRD-pure samples of form II (Fig. 7). The nature of splitting has not been determined, only it can be pointed out that when a heating process is interrupted at the minimum point between two peaks and followed by fast cooling to ambient temperature, the second maximum at $t = 588$ °C during the repeated heating process does not appear. Melting of form I (effect with a maximum at $t = 655$ °C on Fig. 1 and $t = 651$ °C on Fig. 7) also lacks a simple phase transition.

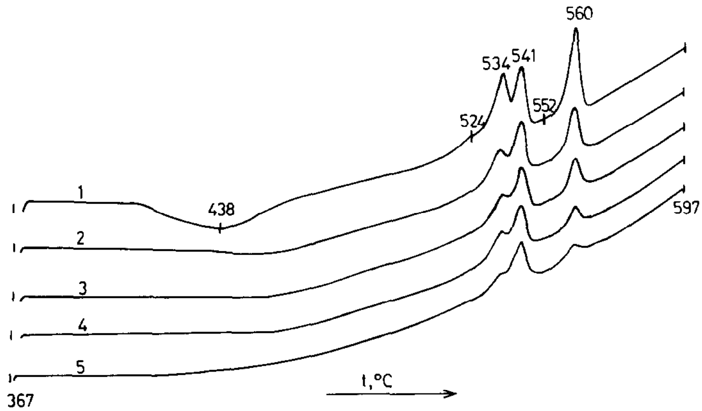

Fig. 8. DSC curves for the heating process of a vitreous sample of overall penta-sodium triphosphate composition in dry nitrogen flow ($m = 9.40$ mg): 1, 2, 3, 4, 5 represent the first, second, third, fourth and fifth cycles of heating to 597 °C (HR = 20 K min^{-1}) with cooling to 367 °C (CR = 320 K min^{-1}).

It is known that the melting of the chain-triphosphate is associated with anion rearrangement and formation of a melt with a certain anion distribution. The distribution function depends on the heating rate, temperature, isothermal treatment time and other factors. A sample of form I on heating to $t = 647$ °C with a heating rate of HR = 80 °C min^{-1} and on cooling to 50 °C at a cooling rate of CR = 320 °C min^{-1} from TLC data contains: 2.0% P_1, 33.9% P_2, 46.3% P_3, 3.4% $P_4 + P_5 + P_6 + P_7$ (phosphorus in the form of chain tetra-, penta-, hexa- and heptaphosphates, respectively), 14.3% P_{start} (phosphorus at the start of the chromatogram), and from the XRD data crystalline phases $Na_4P_2O_7$ and $Na_5P_3O_{10}$-I. It represents a vitreous mass containing crystalline particles of $Na_4P_2O_7$ and $Na_5P_3O_{10}$-I.

On heating the vitreous mass below the glass-softening temperature, the DSC curve showed effects which correspond to the phase transition between the enantiotropic forms of $Na_4P_2O_7$ (Fig. 8). With an increased number of heating–cooling cycles, these effects gradually disappear, as a result of the interaction of $Na_4P_2O_7$ with a glass and its transformation into the chain-triphosphate, whose content increases (Table 1). When the above cycles were repeated in the temperature range 367–597 °C, the chain-triphosphate accumulated in the sample in the form of $Na_5P_3O_{10}$-I, and in the range 367–457 °C in the form of $Na_5P_3O_{10}$-II. In the latter case the sample contains a constant amount of stable form I, which is obtained during glass formation from the melt, and an increasing amoung of form II.

At temperatures preceding melting of the whole sample of $Na_5P_3O_{10}$-I, some physical and chemical processes take place which influence the shape of the heating–cooling DSC curves.

In the range of premelting temperatures the powder-like sample gradually changes its apparent density with increasing temperature but without a

TABLE 1

Content of anion components in the vitreous sample of overall penta-sodium triphosphate composition, which was exposed to heating–cooling cycles in the range 367–597 °C

Number of cycles	Phosphorus content (mass%) as			
	P_1	P_2	P_3	$P_4+P_5+P_6+P_7+P_{start}$
2	0	18.9	68.5	12.6
3	0	12.8	81.3	5.9
4	1.7	12.0	80.1	6.2
5	0.6	9.6	85.2	4.5

change in anion composition (Table 2). The transformation of anion begins and accelerates when the particles of the powder start to sinter, forming at first a weak, and at a later stage a harder and harder conglomerate. Further behavior of a sample depends on the materials of the pan: in the gold pan, conglomerate and melt form a flat thin layer; and in the graphite pan the conglomerate forms a sphere, and the melt almost forms a spherical drop. The obvious sphere of the conglomerate is composed of the outer melt layer and the inner part which represents a weak unit of the powder. From the TLC data of one of the conglomerates, the outside melt layer contains: 2.8% P_1, 23.3% P_2, 65.2% P_3, 8.7% $P_4 + P_5 + P_6 + P_7 + P_{start}$, and the inner powder-like nucleus of a conglomerate: 2.2% P_1, 6.6% P_2, 82.0% P_3, 9.2% $P_4 + P_5 + P_6 + P_7 + P_{start}$.

A similar variation in the physical state of a sample could be observed using DSC (Fig. 9). The temperature of a sample, after preliminary heating at 80°C min^{-1} to 527°C, is changed in a cyclic manner with the next program (graphite pan): temperature increase to 623°C with HR = 80°C min^{-1}, followed by next heating step to $t_{x=1}$ with HR = 1.25 K min^{-1}, and

TABLE 2

The change of physical state and anion composition for $Na_5P_3O_{10}$-I at the premelting and melting temperatures (heating process is carried out to t_x (°C) with heating rate, HR = 10 K min^{-1}, and cooling with rate, CR = 320 K min^{-1})

Physical state at t_x	t_x	Phosphorus content (mass%) as			
		P_1	P_2	P_3	$P_4+P_5+P_6+P_7+P_{start}$
Powder	600	0	0	100	0
Settled powder (higher value of apparent density)	610	0	0	100	0
Weak sintered powder	620	trace	11.1	85.8	3.1
Melt	630	trace	28.3	63.3	8.4
Melt	660	trace	57.9	26.6	15.5

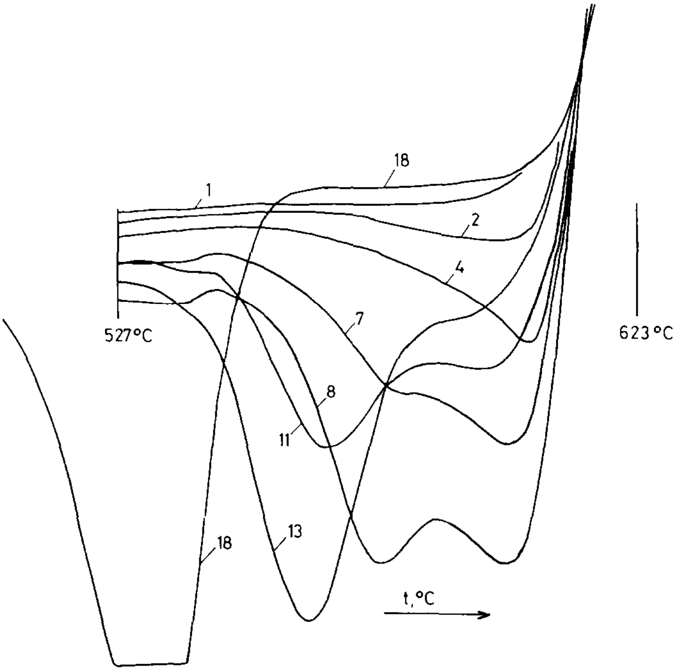

Fig. 9. Parts of the DSC curves of cooling of $Na_5P_3O_{10}$-I in cycles:

$$527\,°C \xrightarrow{HR = 80\ K\ min^{-1}} 623\,°C \xrightarrow{HR = 1.25\ K\ min^{-1}} t_x \xrightarrow{CR = 80\ K\ min^{-1}} 527\,°C$$

(m = 14.85 mg, dry nitrogen flow, graphite pan), numbers of curves on the figure are the same as the number of the cycles explained in Table 3.

TABLE 3

Program for the cyclic change of the end temperature, t_x, in the series of heating and cooling processes for $Na_5P_3O_{10}$-I:

$$527\,°C \xrightarrow{HR = 80\ K\ min^{-1}} 623\,°C \xrightarrow{HR = 1.25\ K\ min^{-1}} t_x \xrightarrow{CR = 80\ K\ min^{-1}} 527\,°C$$

x	t_x (°C)	x	t_x (°C)
1	623	10	629
2	625	11	630
3	625.5	12	631
4	626	13	632
5	626.5	14	633
6	627	15	634
7	627.5	16	635
8	628	17	637
9	628.5	18	677

cooling at CR = 80 °C min^{-1} to 527 °C. The cycle was repeated successively to different temperatures ($t_{x=2}$, $t_{x=3}$, etc.). Series of temperatures, t_x, are shown in Table 3.

In the range of the first heating–cooling cycle, the effect characteristic of vitrification of the melt does not appear in the DSC curve, only a settling effect of the powder sample is observed. This effect appears at the end of the second cycle, and becomes more pronounced in relation to the number of repeated cycles. It then splits and becomes the only effect of the whole sample's vitrification. This last one is shown in the case of the 18th cycle, after which cooling is prolonged below $t = 527$ °C. It corresponds to the effect of glass formation from a whole melted sample of $Na_5P_3O_{10}$-I which is represented in Fig. 7 (I′). The cooling process of the sample after the 18 repeated cycles gives only a glass sphere.

The effects of splitting during heating–cooling cycles have not been observed in the case of the gold pan. This phenomenon could be attributed to the physical process of development of the sphere conglomerate from the initial powder sample in the graphite pan during DSC analysis. At first, the formation of a glassy layer on the outside of the conglomerate is recordered. The glass formation into the core of the conglomerate is then observed. Between the surface layer and the core there is a different anion composition. It is necessary to emphasize that the influence of the pan material on the results of DSC analysis is limited to the temperature range just before or at melting. At other temperatures this influence is not observed. The same results have been obtained with graphite, gold, platinum and aluminum pans in the case of $Na_5P_3O_{10} \cdot 6H_2O$ dehydration. The aluminum pan has an advantage over other materials, because after encapsulation, investigation in an autogenerated atmosphere could be carried out.

CONCLUSION

Iso- and non-isothermal behaviors of the sodium chain-triphosphate hexahydrate, $Na_5P_3O_{10} \cdot 6H_2O$, which has been investigated using DSC, TG, EM, quantitative TLC and XRD methods in the range 50–726 °C, have some particular characteristics, which are different from the thermal behavior of sodium cyclo-triphosphate hexahydrate, $Na_3P_3O_9 \cdot 6H_2O$. With increasing temperature the dehydration process of $Na_5P_3O_{10} \cdot 6H_2O$ has been followed by the transformation $Na_5P_3O_{10}$-II → $Na_5P_3O_{10}$-I and then melting of $Na_5P_3O_{10}$-I. Processes of dehydration and melting proceed via anion rearrangement. Dehydration consists of four steps: removal of 2/6 of the initial water in kinetic ($\Delta m < 0.6$ mol H_2O) and diffusion regimes ($\Delta m = 0.6$–2.0 mol H_2O) without degradation; hydrolytic degradation to the mono- and di-phosphates ($\Delta m = 2.0$–5.0 mol H_2O), and recondensation of the anion of the last compounds to $Na_5P_3O_{10}$-II ($\Delta m = 5.0$–6.0 mol H_2O). The products of degradation of $Na_5P_3O_{10} \cdot 6H_2O$ in contrast to the products of decyclization of $Na_3P_3O_9 \cdot 6H_2O$, do not react with gaseous ammonia.

In the region before melting and for melting temperatures of $Na_5P_3O_{10}$-I, a characteristic effect was observed, which depends on the pan material and could be explained due to a change in physical state and the changed anion composition of the sample.

REFERENCES

1 H.M. Ondik and J.W. Gryder, J. Inorg. Nucl. Chem., 14 (1960) 240.
2 S.I. Pytlev and E.A. Prodan, Izv. Akad. Nauk SSSR, Neorg. Mater., 21 (1985) 976 (in Russian).
3 E. Thilo, Über den Mechnismus der Kristallwasserabgabe aus Kondensierten Phosphaten, Akademia, Berlin, 1952, 16 pp.
4 E.A. Prodan, L.I. Prodan and N.F. Ermolenko, Tripolifosfaty i Ikh Primenenie (Tripolyphosphates and Their Use), Nauka, Minsk, 1969, 533 pp. (in Russian).
5 R.K. Osterheld, Topics in Phosphorus Chemistry, Vol. 7, Wiley, New York, 1972, p. 103.
6 W.O. Groves and J.W. Edwards, J. Phys. Chem., 65 (1961) 645.
7 E.A. Prodan, M.M. Pavlyuchenko and S.A. Prodan, Zakonomernosti Topokhimicheskikh Reaktsij (Principles of Topochemical Reactions), Nauka i Tekhnika, Minsk, 1976, 261 pp. (in Russian).
8 A.J. Mabis and O.T. Quimby, Anal. Chem., 25 (1953) 1814.